DOI: 10.31577/ahs-2023-0024.01.0012

ACTA HYDROLOGICA SLOVACA

Volume 24, No. 1, 2023, 101 – 112

Water erosion mapping using several erosivity factors in the Macta Basin (North-West of Algeria)

Khadidja SEMARI, Khaled KORICHI*

The quantification of the water erosion using empirical models has been applied for several regions around the world. Indeed, the model proposed by Wischmeier and Smith also called RUSLE model remains the most used approach. The main purpose of this work is to produce a soil losses vulnerability map of the Macta Basin and to determine its water erosivity potential, taking into account four rainfall erosivity indices that have been widely applied in the Mediterranean regions namely: Arnoldus index, MFI Modified Fournier Index, Roose index and Rango-Arnoldus index. The calculation of soil losses with the RUSLE model gives respectively the values: 7.94, 13.98, 12.5 and 20.6 t ha^{-1} $year^{-1}$. By comparing with other basins of the same characteristics, we note a good correlation.

KEY WORDS: Macta Basin, Water erosion, Rainfall erosivity, RUSLE, Soil loss

Introduction

The water erosion process at the catchment scale is characterized by three phases, namely: the tearing phase, the transport phase and the deposit or sedimentation phase. Downstream of the watershed, the storage capacity of the dams is reduced under the siltation effect, this is the case of the Fergoug dam in the wilaya of Mascara (North West of Algeria). Upstream of the watershed, there will be land losses, which causes a drop in agricultural production. The and losses vary from country to other but many work show that erosion is accelerated in the Maghreb countries.

In Algeria, and like most semi-arid zones, the consequences of water erosion are disastrous, offering a naked landscape and crisscrossed by an intense ravine, particularly in mountainous regions with a dense hydrographic network. The operational dams are therefore threatened, especially in the west of Algeria, given that 47% of all of its land is affected (Kouri, 1993; Gomer, 1992; Touaïbia, 2000). In Morocco, cumulative annual land losses are estimated at 100 million tons (Heusch, 1970). In Tunisia, water erosion totals 8.5 million hectares which represents 52% of the total country area (Cormary and Masson, 1964).

The intensity of water erosion depends on the climatic conditions, hence the rains erosivity, the slope which acts directly on the kinetic energy of the runoff, the cover land which absorbs the energy kinetics of the raindrops and increases the soil resistance against erosion, and finally soil erodibility which is closely related to the texture and soil structure.

To estimate and quantify water erosion, several scientific approaches are proposed in the literature. The simplest empirical models are applied only for sufficiently large spatiotemporal scales. More elaborate mechanistic models that estimate the spatial distribution of solid fluxes for each meteorological event. However, the availability and the quality of data required to estimate the risk of water erosion remains a real challenge especially in large ungauged catchments, but with the rapid development of GIS tools, empirical models have become more effective approaches and thus constitute a better decision-making tool.

Empirical models are hydrological models based on mathematical laws applied and validated in the laboratory or on experimental fields. The simplest and most widely used model, which relates soil loss to rainfall or runoff is governed by the Universal Soil Loss Equation (USLE) and carried out by (Wischmeier and Smith 1965; 1978). The modified version of the model, proposed by (Williams, 1975), estimates the solid transport of each storm by taking into account the volume of runoff instead of the rain erosivity (Djoukbala et al, 2018).

In this work we are interested in the mapping of the vulnerability to water erosion expressed in soil losses in the Macta Basin. A parametric investigation of the erosivity is thus carried out using four empirical formulas dedicated to Mediterranean semiarid catchments with ephemeral streams called also Wadis, to estimate their effects. The Macta Basin is characterized

by a long period of drought, over the period 1930–2002, from which annual rainfall recorded a drop of around 40% on average (Meddi et al, 2009), adding the predominance of silt and clayey-sandy textures. The consequences of water erosion are manifested by the siltation of the Fergoug dam located downstream of the Macta Basin. The mapping of areas with high water erosion requiring development has become essential to minimize the rate of siltation.

Materials and Methods

Study area

Located in the North-West of Algeria, the Macta Basin extends over an area close to 14400 km^2. It is limited to the North by the Mediterranean Sea, to the South by the Oran highlands, to the East by the Cheliff Zahrez region and to the West by the Tafna catchment and the Oran coast (Fig. 1).

The Macta Basin encompasses two representative sub-basins: Mekerra and Wadi El Hammam over which two main streams flow:

1. The Wadi Mekerra covers a distance of 115 km and takes its source from Ras El-Ma, precisely, in the heights of Djebel El-Beguira at an altitude of 1402 m, 86 kilometers from the center of Sidi Bel Abbes city. The Wadi Mekerra crosses obliquely, from the South-West to the North-East, dozens of rural and urban perimeters before flowing into the Macta marshes and then into the Mediterranean Sea (Semari and Benayada, 2019).
2. The Wadi El Hammam rises 16 km south-west of Ras El Ma at an altitude of 1100 m and travels 172 km in the south-east direction. It is formed by the confluence of three Wadis: Melrir, Hounet and Sahouet which join at the point named Trois Rivières (Fig. 1).

The Macta Basin is subject to the semiarid climate characterized by a cold winter and hot summer, it undergoes the Mediterranean influence in the North and the continental conditions in the South from where the precipitations are irregular in space and in time.

The northern borders where the marshes are located and the southern limits of the Macta Basin are characterized by low slopes which vary between 0 and 9%. Upstream of the marshes, most of the areas have steep slopes between 40 to 58%. To the east, the slopes range between 18 and 47%, while in the West the slopes are moderate and do not exceed 27% (Fig. 2).

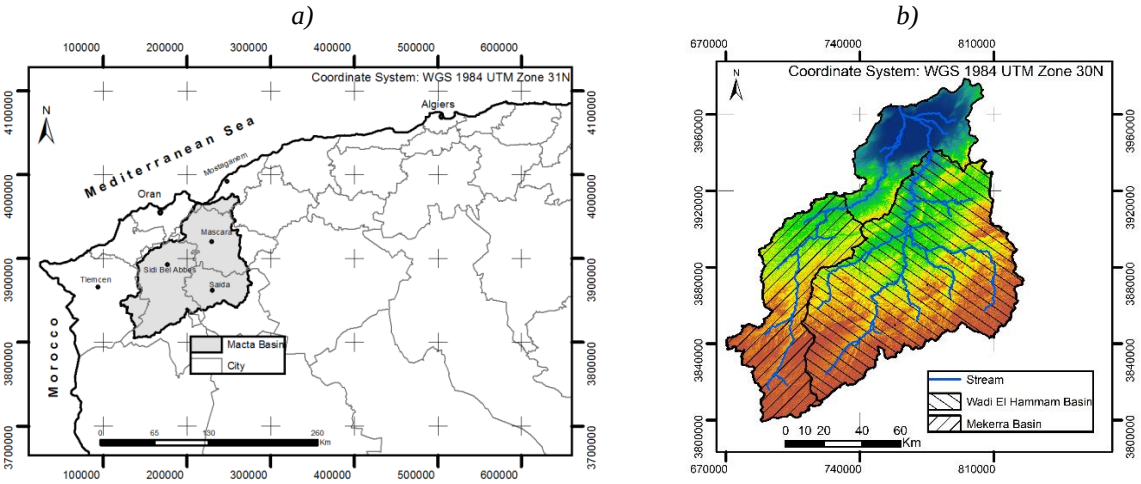

Fig. 1. a) Geographic location of the Macta Basin, b) sub-basins and hydrographic network.

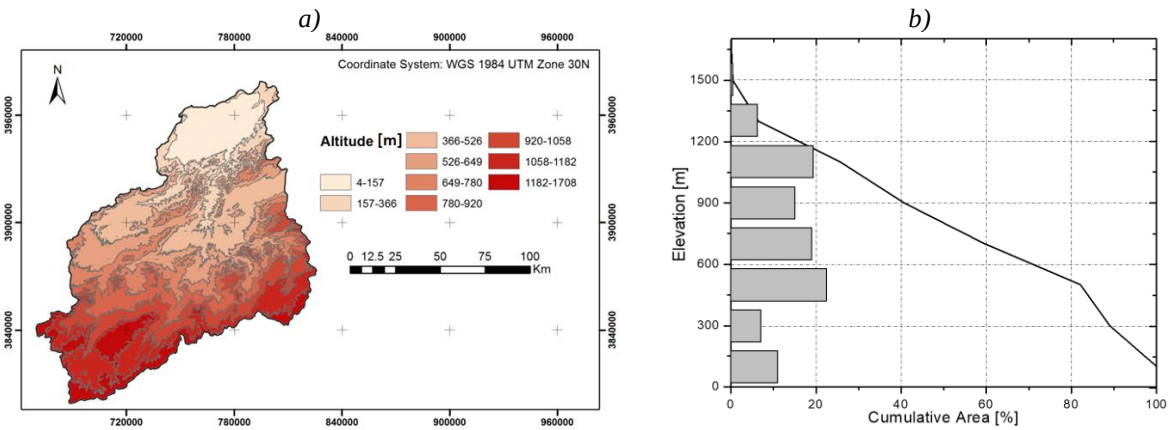

Fig. 2. a) Level curves map of the Macta Basin, b) Hypsometric curve.

The relief of the Macta Basin is characterized by the existence of plains interspersed with massifs:

- *Low coastal plain:* It is separated from the sea by a band of dune and has altitudes below 9 m. We notice the presence of water bodies, marshes and more or less humid steppes. Upstream, the plain extends to the southeast through the valleys of the Wadis of Sig and Habra.
- *Plain of Ghriss*: is located in the sub-basin of Wadi El Hammam and drained by Wadi Fekane. It is limited to the north by the mountains of Beni-Chougrane, to the south by the mountains of Saïda, to the west by the valley of Wadi Melrir. The average altitude is 500 m. It has no outlet to the sea; which has favored the frequent presence of floodplains.
- *Plain of Sidi Bel Abbes:* Located in the sub-basin of Wadi Mekerra. It is bordered to the north by the Tessala Mountains, to the south by the Tlemcen and Saïda mountains, to the west by the Wadi Isser valley and to the east by the Beni-Chougrane Mountain chain. The plain of Sidi Bel Abbes is classified as flood prone.
- *Beni-Chougrane's mountains:* They separate both plains of the Mascara province; the peak can reach 910 m. These massifs are covered by forests and scrubland or maquis which are subject to degradation linked to soil erosion and the intensity of human activity.
- *Mountains of Tessala*: constitute a complex massif of an average altitude of 800 m, where the highest point reaches 1061 m. They are crossed by the Mebtouh Wadi before it joins the lower low plain. They limit the Macta Basin to the West and North-West. In the South-West, the Tessala Mountains are relayed by the eastern part of the Tlemcen Mountains.

According to Strahler (1952), the hypsometric curve can give indications on the dynamic equilibrium state of the watershed. The shape of the hypsometric curve (Fig. 2) shows that the Macta Basin is an erosive basin which presents non-equilibrium (young) stage.

Data collection

Fig. 3 schematizes the flowchart of the followed operations to estimate the soil losses in the Macta Basin. The used data are from different sources (Fig 3.) and have been projected in the WGS 84 system, UTM zone 30. One cites:

1. Climate data provided by the National Agency of Hydraulic Resources (NAHR) from forty-two (42) gauge stations distributed throughout the Basin, for a study period which extends from 1967 to 2011 (Fig. 4).
2. Soil data was provided from Harminised World Soil Database HWSD.
3. Topographic data with (30m x 30 m) resolution from SRTM (Shuttle Radar Topography Mission).
4. Satellite images from Landsat 8 (2007) to see the evolution of the density of the vegetation cover.

All the collated data were used to estimate the parameters defied below of the Revised Universal Soil Loss Equation. Data processing was carried out with the ArcGis V.10.4 geographic information system.

RUSLE model factors

The model proposed by Wischmeier and Smith (1965; 1978) is the most commonly used for the quantification of soil losses. This model requires available data on the watershed such as topography, soils, rainfall, landcover, cropping systems and erosion control practices. The Universal Soil Loss Equation (USLE) is written as follows:

$$A = R \times K \times LS \times C \times P \quad (1)$$

where

A is the annual soil loss rate (t ha^{-1} $year^{-1}$);
R is the rainfall erosivity factor expressed in Mega-Joule mm ha^{-1} $hour^{-1}$$year^{-1}$;
K is the soil erodibility factor (t ha $hour^{-1}$$ha^{-1}$$MJ^{-1}$$mm^{-1}$);
LS is a dimensionless factor that represents the slope (S in %) and the length of the slope (L in m);
C is dimensionless factor of plant cover and cropping practices;
P is a dimensionless factor related to land use and the conservation practices.

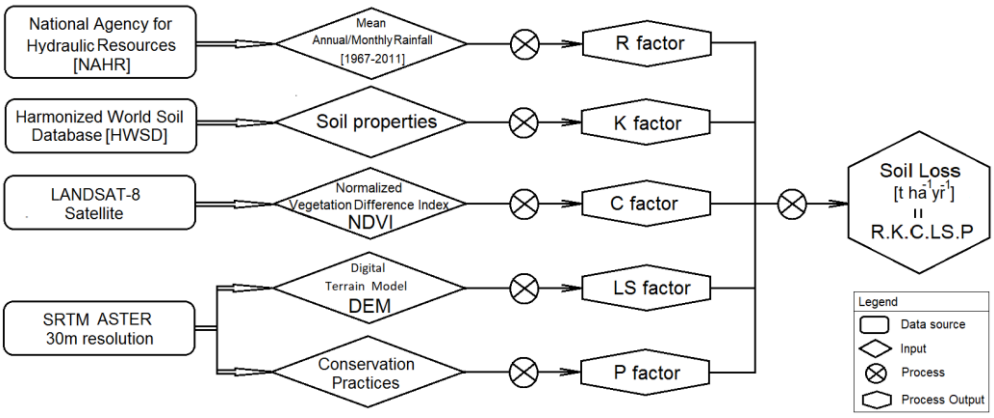

Fig. 3. Methodological flowchart of water erosion mapping.

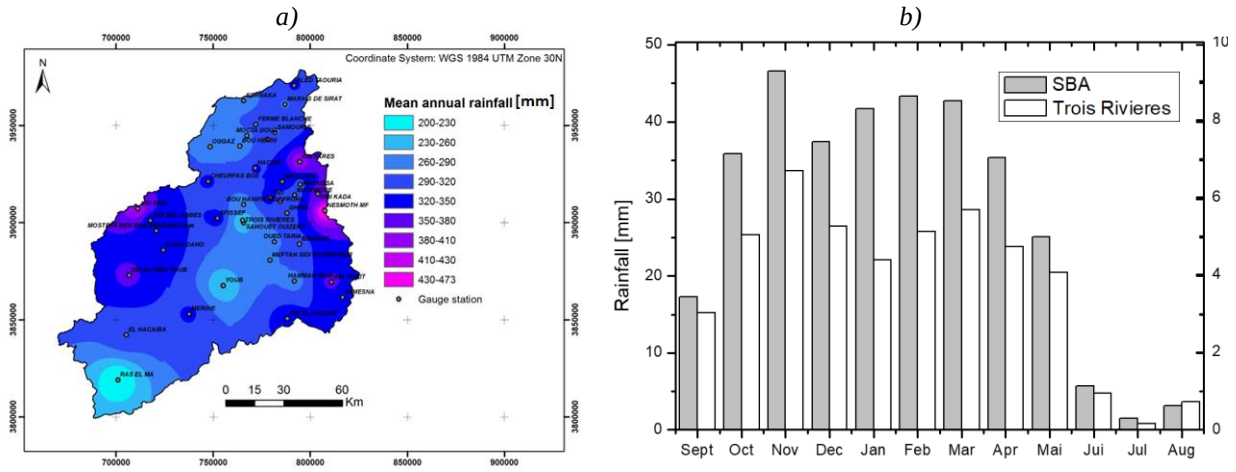

Fig. 4. a) Spatial distribution of average annual precipitation, b) Histogram of monthly precipitation at the stations of Sidi Bel Abbes and the Trois Rivieres.

Rainfall erosivity indices

In the literature, several authors have proposed a variety of rainfall erosivity indices. In this study we are mainly interested in four indices such as: 1) Erosivity index of Arnoldus, 2) Modified Fournier Index, 3) Roose's erosivity index and Rango-Arnoldus index:

Arnoldus Index

The Arnoldus formula (Arnoldus, 1980) translates a linear regression with the Modified Fournier Index according to equation (2).
This combination has been tested and applied in the regions of West Africa.

$$\mathrm{R1} = 0.66\mathrm{MFI} - 3 \tag{2}$$

Modified Fournier Index (MFI)

The (MFI) index proposed by Arnoldus (1980), consists of using the sum of the Fournier indices for the twelve months of the year, it is the sum of the ratio of the squares of the average monthly rainfall and the average annual rainfall.

$$R2 = MFI = \sum_{i=1}^{12} \left(\frac{P_i^2}{P}\right) \tag{3}$$

Roose erosivity index

Roose's work (Roose, 1981), for over than 20 years of measurements, led to the proposal of simple empirical relationships, linking the erosivity index to the average annual rainfall P_{an} for the same period such as:

$$R3 = a\, P_{an} \tag{4}$$

The value of (a) is around 0.1 to 0.12 in northwestern Algeria (Morsli et al, 2004).

Rango-Arnoldus index

An alternative formula, that involves monthly and annual precipitation to determine the R factor, are proposed by Arnoldus (Rango and Arnoldus, 1987). It has been applied by several authors for the quantification of erosion in the Maghreb regions is presented in the form:

$$\mathrm{Log\ R4} = 1.74.\mathrm{Log} \sum \left(\mathrm{Pi}^2/\mathrm{P}\right) + 1.29 \tag{5}$$

where
R4 – is in [MJ mm ha^{-1} hour^{-1} year^{-1}]
Pi and *P* – represents respectively the monthly and mean annual rainfall in [mm]

Soil erodibility factor (K)

This factor reflects the resistance of a soil to water erosion. The *K* factor depends on several properties of the soil in particular; the percentage of sand, silt and clay and also the content of organic matter and permeability. Based on Global Harmonized Soil data version 1.2, one can establish the map of soil properties in the study area. The value of the soil erodibility is calculated using the formula proposed by (Neitsch et al, 2011).

$$K = f_{csand} \cdot f_{cl-si} \cdot f_{orgc} \cdot f_{hisand} \tag{6}$$

where
f_{csand} – decreases the value of *K* in case of high coarse sand content and increases it in case of fine sand soil;
f_{cl-si} – decreases the value of *K* for soils with a high ratio of clay to silt;
f_{orgc} – decreases the value of *K* for soils with high organic matter content;
f_{hisand} – decreases the value of *K* for soils with a very high sand content.

Each parameter is given as:

$$f_{csand} = 0.2 + 0.3.exp\left[-0.256.m_s.\left(1-\frac{m_{silt}}{100}\right)\right] \quad (7)$$

$$f_{cl-si} = \frac{m_{silt}}{m_{silt}+m_c} \quad (8)$$

$$f_{orgc} = 1 - \frac{0.25.orgC}{orgC+exp(3.72-2.95.orgC)} \quad (9)$$

$$f_{hisand} = 1 - \frac{0.7.\left(1-\frac{m_S}{100}\right)}{1-\frac{m_S}{100}+exp\left[-5.51+22.9.\left(1-\frac{m_S}{100}\right)\right]} \quad (10)$$

where

m_s – is the percentage of sand content in where the particle diameter is between 0.05 and 2 mm;

m_{silt} – is the percentage of silt content with particle diameters between 0.002 and 0.05 mm;

m_c – is the percentage of the clay content whose particle diameters are less than 0.002 mm;

$orgC$ – is the percentage of organic carbon content.

Land cover factor (C)

The land cover plays an important role in soil protection, land losses decrease with the increase in the landcover rate. Many studies have been proposed to estimate the *C* factor using the Normalized Vegetation Difference Index (NDVI) (Lin et al., 2002; Wang et al., 2002). Knowing that the vegetation absorbs a significant part of the solar radiation in the red band and it reflects it to the maximum in the near infrared band, this index is determined as follows:

$$NDVI = \frac{PIR-R}{PIR+R} \quad (11)$$

where:

PIR – Numerical value of the same pixel in the near infrared band (between 0.55 and 0.68μm);

R – Numerical value of the same pixel in the red band (between 0.73 and 1.1 μm).

The NDVI value varies between -1 and +1; negative values correspond to surfaces other than plant cover, such as snow, water or clouds for which the reflectance in the red band is greater than that of the near infrared. For bare soils, the reflectance being roughly of the same order of magnitude in the red and the near infrared where the NDVI is close to zero. On the other hand, the plant formations, have positive NDVI values, generally between 0.4 and 0.7. The highest values correspond to very dense plant cover.

NDVI data are obtained from the Landsat-8 satellite. To estimate the C factor, several authors have developed regressions with NDVI (Karaburun, 2010; Ouallali et al, 2016). Since our study area is located in the North-West of Algeria, it is more convenient to select the regression proposed by (Toumi et al, 2013) given as:

$$C = 0.9167 - 1.1667NDVI \quad (12)$$

Topographic factor (LS)

The slope plays a crucial role in the process of uprooting, transport and sediments deposition. Runoff increases with the slope increasing. Several formulas allow the evaluation of the LS factor from the DEM, such as that of Kalman (1967), David (1987) and Mitasova et al. (1996). In our case, we use the formula of (Wischmeier and Smith, 1978) given by:

$$LS = \left(\frac{L}{22.13}^{m}\right)(0.065 + 0.045S + 0.0065S^2) \quad (13)$$

where:

L – is the length of the slope in [m];

S – the inclination of the slope in [%];

m – is a classification parameter such:

m=0.5 if the S >5%,

m=0.4 if 3.5% < S < 4.5%;

m=0.3 if 1< S < 3%,

m=0.3 if S < 1%.

Soil conservation practices factor (P)

The *P*-factor takes into account anti-erosion practices and cultivation techniques used to reduce the runoff effect and erosion. Among these techniques, we find contour farming, the laying of grassy strips between two cultivation areas, natural or artificial mulching, and the laying of cover crops. Based on the work of (Roose, 1994), the P value is determined from the following Table 1.

Table 1. *P*-factor classes (Roose, 1994)

Land-use type	*P*-factor
Degraded bare ground	1
Fallow	1
Big cultures	0.7
Low density forest plantation	0.5
Vegetable crops	0.5
Arboriculture	0.5
Contour ploughing	0.2
Planting on terraces	0.14
Water body	0

Results and discussion:

R-erosivity factor

The erosivity maps generated from the rainfall data of the 42 stations, and using the four empirical formulas give the same erosivity distribution. They thus show that the values of the R1, R2, R3 and R4 factors in the Macta Basin vary from 9.54 (Arnoldus) to 73 (Rango-Arnoldus) MJ mmha^{-1}hour^{-1}year^{-1} (Table 2). The high values are recorded at the eastern and western of the basin borders, while the southern areas indicate lower values (Fig. 5). It can thus be seen that erosivity is directly related to

the precipitation (Fig. 3a), both distribution are well correlated.

The erosivity indices Rare distributed in the Macta Basin into four classes, R1, R2, R3 and R4. With the exception of the Roose index, the other approaches show that the high erosivity class has a low percentage (Table 2), (R1 6.01%, R2 6.49%, R3 18.36%, R4 6.92%). The low erosivity classes also occupy small areas (R1 8.52%, R2 8.45%, R3 8.51%, R4 8.55%). The average erosivity class dominates the surface of the Macta Basin with values from R1 (15.17) to R4 (57.09) MJ mm ha^{-1} $hour^{-1}$ $year^{-1}$. Given the large surface area of the Macta Basin, the range of precipitation values (200–473 mm) is wide enough that the variance is also high and the extrema values (min and max) occupy a small part of the basin.

Table 2. Distribution of R-erosivity factors in the Macta Basin

R1 Arnoldus Classes	Area [ha]	Area [%]	R2 MFI Classes	Area [ha]	Area [%]
9.54–15.17	122640.61	8.52	19–27.53	121721.89	8.45
15.17–18.96	620097.61	43.06	27.53–33.27	600931.66	41.73
18.96–22.39	610638.53	42.41	33.27–38.47	623844.48	43.33
22.39–31.98	86593.27	6.01	38.47–53	93471.97	6.49
Total	1439970	100	Total	1439970	100
R3 Roose Classes	Area [ha]	Area [%]	R4 Rango-Arnoldus Classes	Area [ha]	Area [%]
20–26.35	122497.22	8.51	34–44.45	123063.24	8.55
26.35–30.16	495484.63	34.41	44.45–51.28	597000.94	41.46
30.16–33.45	557624.12	38.72	51.28–57.09	620248.24	43.07
33.45–47	264364.03	18.36	57.09–73	99657.58	6.92
Total	1439970	100	Total	1439970	100

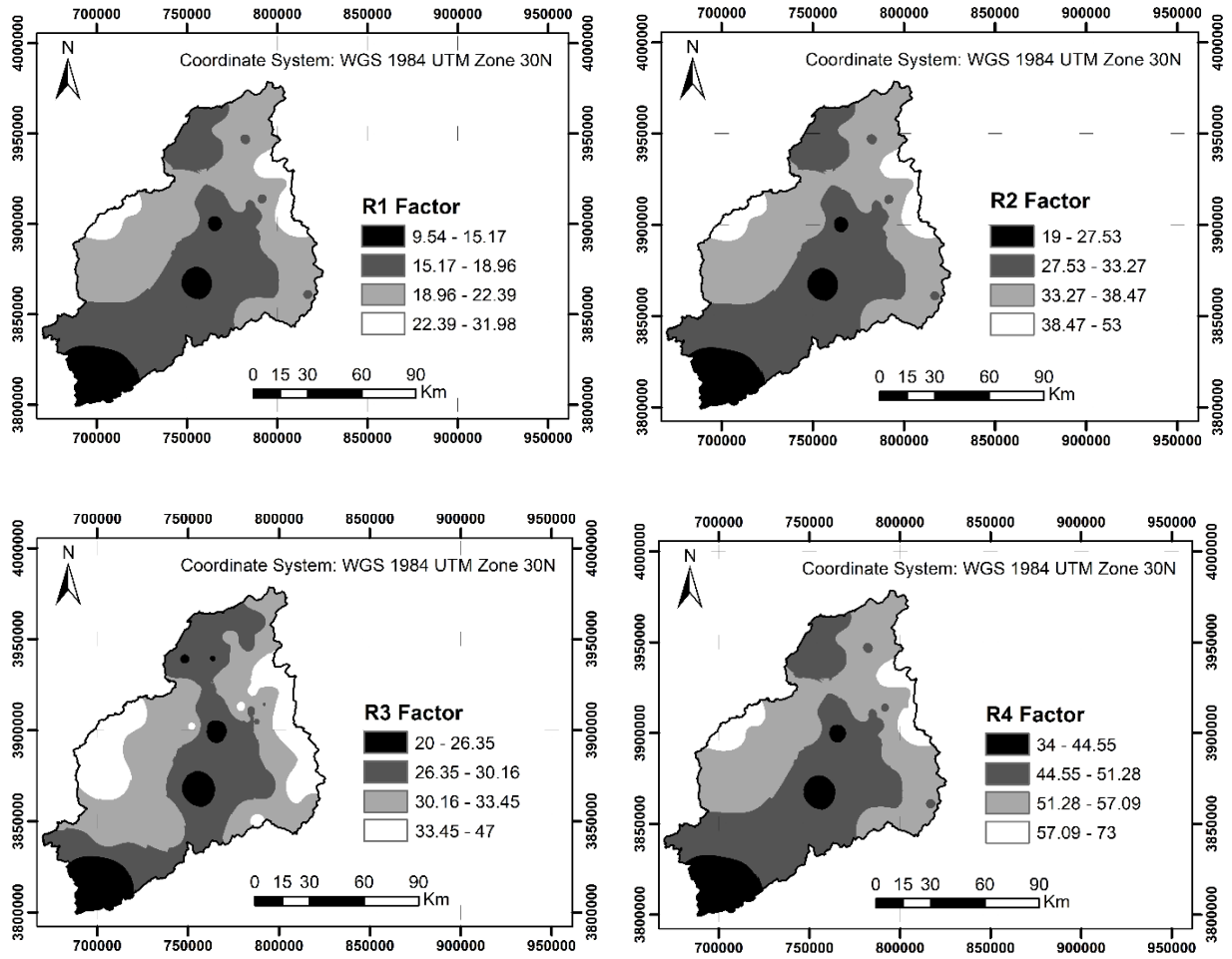

Fig. 5. Spatial distribution of R-erosivity factors in the Macta Basin.

K-erodibilityfactor

Fig. 6a indicates the classification of soils in the Macta Basin, one can see that grazing areas dominate the surface of the basin. The spatial distribution of the erodibility classified into four groups (Fig. 6b) indicates that the soil *K*-erodibility factor in the Macta Basin ranges from 0.0138 to 0.0227 t ha hour MJ^{-1} ha^{-1} mm^{-1}. Almost half of the basin surface (58.35%) has a low *K* index (0.013) Table 3.

C-landcover factor

Using the NDVI map (Fig. 7a), the spatial distribution of the *C*-landcover factor of the Macta Basin is generated using ArcGIS software. The values of C factor observed over the entire study area vary from 0.09 to 1.8. More than 60% of the area of the basin has very low vegetation cover, 8% of the area has a *C* index less than 0.5. Values below 0.5 refer to dense forests, dense scrubland or matorral and arboriculture. Values between 0.5 and 0.9 are assigned to areas covered with sparse forests. Values tending to 1 are related to bare soil and harvested cropland (Table 4).

LS-slope factor

Erosion has been shown to increase exponentially with the degree and length of slope inclination represented by the *LS* factor. The length *L* and the slope *S* are very decisive parameters in the erosion process. Thus, the transport accelerates downward due to the increase in the kinetic energy of the runoff. In the Macta Basin, the distribution of the LS factor has been classified into five groups (Table 5). The highest values of *LS* are noticed from upstream to downstream and show a southwest-northeast orientation; they are mainly concentrated in the eastern side of the Macta Basin (Fig. 8). The *LS* low values are observed in the plain, this corresponds to 1) low altitude areas, concentrated mainly in the western part of the basin, 2) plain areas such as the plains of Ghris, Sidi Bel Abbes and of Mohammadia and 3) to the floodplains of Wadi Mekerra and Wadi El Hammam.

Table 3. Distribution of the *K*-erodibility factor in the Macta Basin

K factor classes	Area [ha]	Area [%]
0.013885	840231.70	58.35
0.01594	433841.30	30.13
0.018043	15355.20	1.07
0.02276	150541.80	10.45
Total	1439970	100

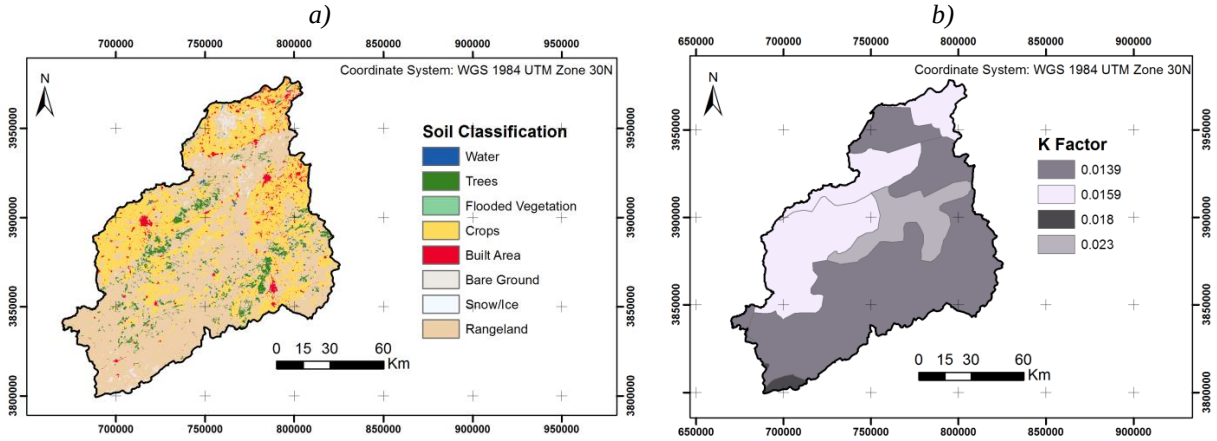

Fig. 6. a) Spatial distribution of soils and b) erodibility factor K in the Macta Basin.

Table 4. Distribution of the *C*-landcover factor in the Macta Basin

Classes *C* factor	Area [ha]	Area [%]
0.09–0.57	121753.27	8.46
0.57–0.66	342287.45	23.76
0.66–0.75	521277.37	36.20
0.75–0.88	450792.44	31.31
0.88–1.18	3859.47	0.27
Total	1439970	100

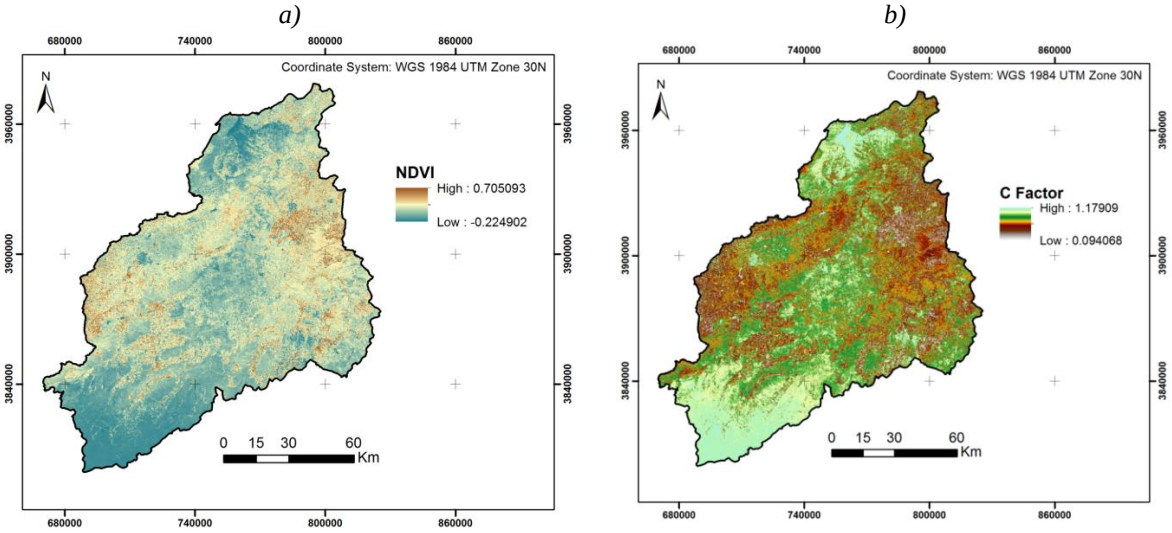

Fig. 7. a) Spatial distribution of NDVI and b) Landcover in the Macta Basin.

Table 5. Distribution of *LS*-factor in the Macta Basin

Classes *LS* factor	Area [ha]	Area [%]
0–0.59	1182214.91	82.10
0.59–2.95	197462.31	13.71
2.95–7.37	45151.38	3.14
7.37–15.33	12823.29	0.89
15.33–75.17	2318.11	0.16
Total	1439970	100

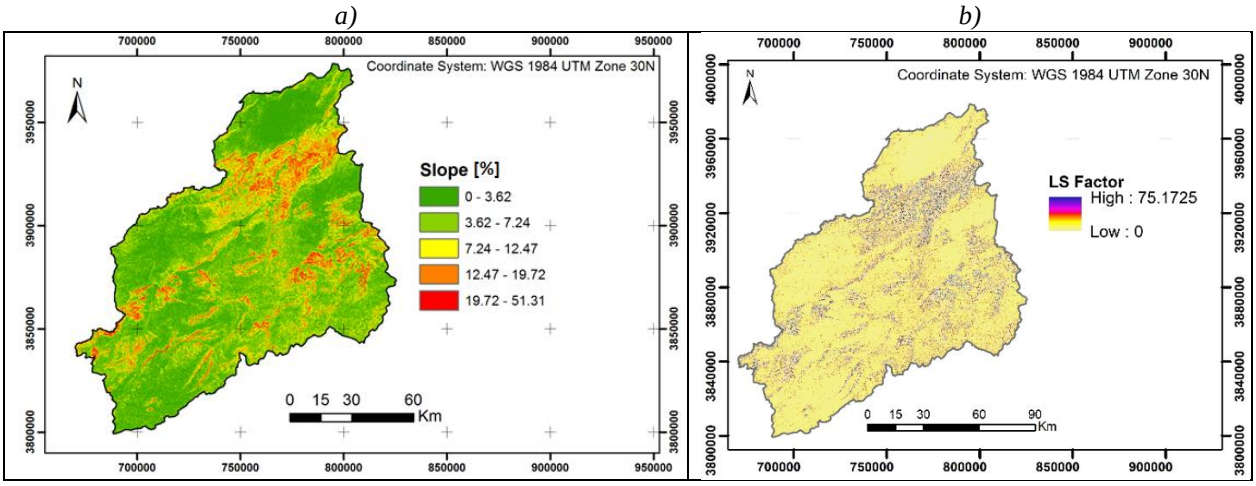

Fig. 8. a) Spatial distribution of the slope [%] and b) LS-slope factor in the Macta Basin.

P-Occupation factor

The *P*-factor takes into account control practices that reduce the erosion potential of runoff in terms of its concentration, velocity and hydraulic forces applied on the soil surface. Support practices include contour tillage, strip-cropping on the contour, and terrace systems. Table 6 summarizes the *P* values in hectares and in [%]. It can be seen that the maximum values coincide with those of the steep slopes following the southwest-northeast orientation (Fig. 9).

RUSLE Soil loss

The average annual soil losses in the Macta Basin have been calculated with the RUSLE model using the four

empirical erosivity formulas discussed above. The erosivity factors are calculated from rainfall data from 42 stations over 45 years (1967–2011). The vector product of the five factors is produced using ArcGIS software and gives a spatial resolution matrix of 30 m x 30 m. These are the four maps showing average soil losses in [t $ha^{-1}year^{-1}$] (Fig. 10). The soil loss classes are summarized in Table 7, from which the mean values are respectively; 7.94, 13.98, 12.5 and 20.6 t ha^{-1} $year^{-1}$. We notice that the model calculated based on R1 Arnoldus indices, underestimates the value of RUSLE, on the other hand the RUSLE obtained by R4 Rango-Arnoldus indices overestimates the soil losses. The results obtained with the R2 (MFI-indices) and R3 (Roose index) show a good correlation with other Algerian basins with similar climatic and environmental characteristics and extracted from the literature, such as 1) the Wadi Mina 11.2 t $ha^{-1}year^{-1}$ (Benchettouh et al., 2017); 2) Wadi Boumahdane basin of 11.18 t ha^{-1} $year^{-1}$ (Bouguerra et al., 2017); 3) basin of the Wadi Sahouat between 12 and 16 t ha^{-1} $year^{-1}$ (Toubal et al., 2018) and 4) Wadi Gazouana between 9.65 and 11.33 t ha^{-1} $year^{-1}$ (Djoukbala et al., 2018).

Table 6. Distribution of *P*-occupation factor in the Macta Basin

Classes *P* factor	Area [ha]	Area [%]
0–0.55	1045732.62	72.62
0.55–0.78	215552.53	14.97
0.78–1	178684.85	12.41
Total	1439970	100.00

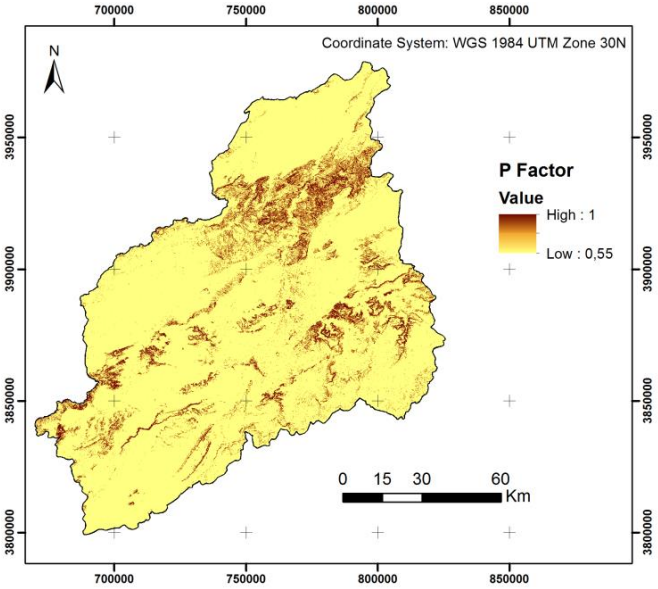

Fig. 9. Spatial distribution of the P-factor in the Macta Basin.

Table 7. Distribution of the soil losses in Macta Basin

RUSLE 1 Classes	Mean [t $ha^{-1}year^{-1}$]	Area [ha]	Area [%]	RUSLE 2 Classes	Mean [t ha^{-1} $year^{-1}$]	Area [ha]	Area [%]
0–0.17		1384676.68	96.16	0–0.65		1384892.62	96.18
0.17–1.35		41548.26	2.89	0.65–2.38		41359.33	2.87
1.35–3.32	7.94	10670.31	0.74	2.38–5.84	13.98	10656.94	0.74
3.32–15.69		3074.75	0.21	5.84–27.59		3061.11	0.21
Total		1439970	100	Total		1439970	100
RUSLE 3 Classes	Mean [t ha^{-1} $year^{-1}$]	Area [ha]	Area [%]	RUSLE 4 Classes	Mean [t ha^{-1} $year^{-1}$]	Area [ha]	Area [%]
0–0.60		1384897.75	96.18	0–1.01		1385826.75	96.24
0.60–2.19		41377.58	2.87	1.01–3.72		40656.30	2.82
2.19–5.39	12.5	10630.94	0.74	3.72–8.96	20.6	10411.98	0.72
5.39–25.44		3063.73	0.21	8.96–43.14		3074.97	0.21
Total		1439970	100	Total		1439970	100

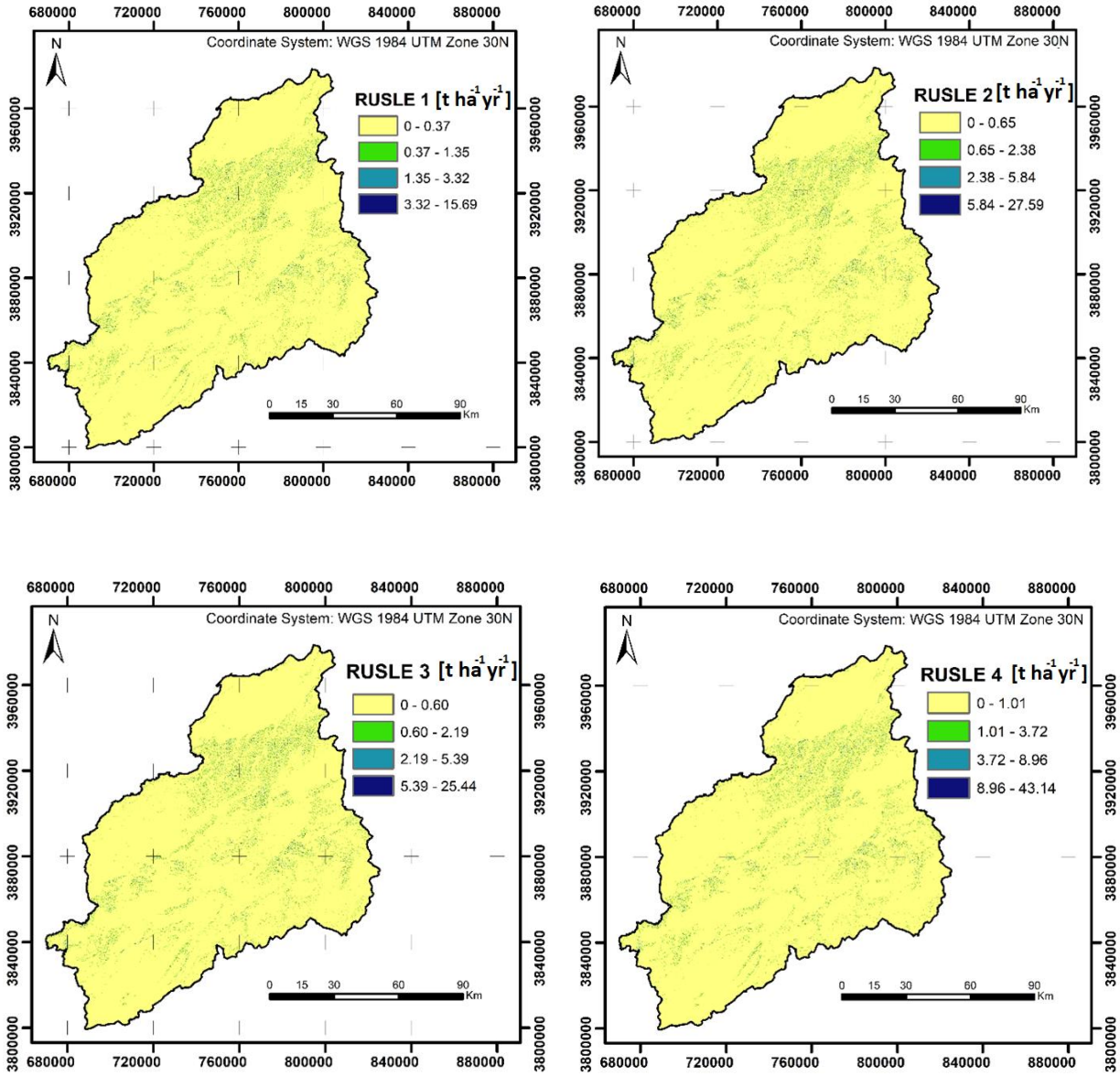

Fig. 10. Spatial distribution of different soil loss in the Macta Basin.

Conclusion

This study focuses on the estimation of soil losses by water erosion in the Macta Basin located in northwest Algeria using the Revised Universal Soil Loss RUSLE model proposed by Wischmeier and Smith. The spatial distribution of the soil losses is thus parameterized using four empirical erosivity factors; (Arnoldus, MFI, Roose and Rango-Arnoldus) and indicates an average values of 7.94, 13.98, 12.5 and 20.6 t ha^{-1} $year^{-1}$ respectively. With the exception of the value calculated using Rango-Arnoldus indices (20.6 t ha^{-1} year-1) and by comparing with other similar Algerian basins, the calculated results are in good agreement. These results also show that about 0.21% of the surface of the watershed has a higher erosion rate, greater than 5 (t ha^{-1} $year^{-1}$), observed on the hills and lands characterized by steep slopes of the catchment. This explains the severity of the soil degradation especially upstream of the Macta Basin due to the lithology, aggressive climate but also unfavourable land use.

Erosion maps, obtained from the four erosivity approaches, provide useful information for selecting suitable areas for planning conservation and preservation works. The modeling of soil loss remains an investigation subject given the complexity of natural phenomena and the non-linearity of the relationships between the intervening variables. However, the use of empirical models is still part of the decision-making tools. It thus has several advantages in terms of mitigating risk with perimeters protection and also to predict soil protection

scenarios by planning intervention works to fight against the phenomenon of water erosion.

References

Arnoldus, H. M. J. (1980): An Approximation of the Rainfall Factor in the Universal Soil Loss Equation. In: De Boodt, M. and Gabriels, D., Eds., Assessment of Erosion, John Wiley and Sons, New York, 127–132.

Benchettouh, A., Kouri, L., Jebari, S. (2017): Spatial estimation of soil erosion risk using RUSLE/GIS techniques and practices conservation suggested for reducing soil erosion in Wadi Mina watershed (northwest, Algeria). Arab J Geosci. https://doi.org/10.1007/s12517-017-2875-6

Bouguerra, H., Bouanani, A., Khanchoul, K. Derdous, O., Tachi, S. (2017): Mapping erosion prone areas in the Bouhamdane watershed (Algeria) using the Revised Universal Soil Loss Equation through GIS. J Water LandDev 32:13–23. https://doi.org/10.1515/jwld-2017-0002

Cormary, Y., Masson, J. (1964): Etude de conservation des eaux et du sol au Centre de Recherches du Génie Rural de Tunisie: application à un projet-type de la formule de perte de sols de Wischmeier. Cahiers ORSTOM, série pédologie 2.3:3–26. ISSN 0029-7259 (in french).

David, W. P. (1987): Soil and water conservation planning. Policies, Issues and recommendations. DENR Quezon City. Journal of Philippine Development, N26, Volume 15, 47–84.

Djoukbala, O., Hasbaia, M., Benselama, O., Mazour, M. (2018): Comparison of the erosion prediction models from USLE, MUSLE and RUSLE in a Mediterranean watershed, case of Wadi Gazouana (N-W of Algeria). Model. Earth Syst.Environ. https://doi.org/10.1007/s40808-018-0562-6

Gomer D. (1992): Ecoulement et érosion dans des bassins versants à sols marneux sous climat semi-aride méditerranéen. GTZ - ANRH 1992; 207 p (in french).

Heusch, B. (1970): L'érosion dans le Prérif: Une étude quantitative de l'érosion hydraulique dans les collines marneuses du Prérif occidental. Annales des recherches forestières, 12, 9–176 (in french). https://doi.org/10.1080/01431160110114538

Kalman, R. (1967): Essai d'évaluation pour le pré-Rif du facteur couverture végétale de la formule de Wischmeier de calcul de l'érosion. Rapport pour l'administration de la forêt et d'eau, Rabat, 1–12 (in french).

Karaburun, A. (2010): Estimation of C factor for soil erosion modeling using NDVI in Buyukcekmece watershed. Ozean Journal of Applied Sciences 3(1) (in french).

Kouri, L. (1993): L'érosion hydrique des sols dans le bassin versant de l'oued Mina. Etudedes processus et type de fonctionnement des ravins dans la zone des marnes tertiaires (in french). PhD Theisis,University of Louis Pasteur, Strasbourg, France.

Landsat 8 (2007): https://earthexplorer.usgs.gov/

Lin C.-Y., Lin W. T., Chou W. C. (2002): Soil erosion prediction and sediment yield estimation: the Taiwan experience. Soil Tillage Res68:143–152. https://doi.org/10.1016/S0167-1987(02)00114-9

Meddi, M., Talia, A., Martin, C. (2009): Evolution récente des conditions climatiques et des écoulements sur le basin versant de la Macta (Nord-ouest de l'Algérie). Physio-Géo – Géographie Physique et Environnement, vol III (in french).

Mitasova, H., Hofierka, J., Zlocha, M. (1996): Modeling topographic potential for erosion and deposition using GIS. International Journal of Geographical Information Science. 10, 629–641.

Morsli, B., Halitim, A. Roose, E. (2004): Effet des systèmes de gestion sur le ruissellement,l'érosion et le stock de Carbone ; du sol dans les monts de Beni-Chougrane (Algérie). Bull RéseauErosion, IRD France, 23: 416–430 (in french).

Neitsch, S., Arnold, J., Kiniry, J., Williams, J. (2011): Soil & water assessment tool theoretical documentation version 2009. Texas Water Resources Institute, 1–647

Ouallali, A., Moukhchane, M., Aassoumi, H., Berrad, F., Dakir, I. (2016): Evaluation and mapping of water erosion rates in the watershed of the Arbaa Ayacha River (Western Rif, Northern Morocco). Bulletin de l'Institut Scientifique, Rabat, Section Sciences de la Terre, 38, 65–79 (in french).

Rango, A., Arnoldus, H. M. J. (1987): Aménagement des bassins versants. Cahiers techniquesdela FAO.

Roose, E. (1981): Dynamique actuelle de sols ferralitiques et ferrugineux tropicaux d'Afrique Occidentale. Étude expérimentale des transferts hydrologiques et biologiques de matièressous végétation naturelles ou cultivées. ORSTOM, Paris (France). Collection travaux et docu-ments, no 130, Thèse d'État Orléans. 569 p (in french).

Roose, E. (1994): Introduction à la gestion conservatoire de l'eau, de la biomasse et de la fertilité dessols (GCES) Bull. Pédol. FAO, 70, 420 p (in french).

Semari, K., Benayada, L. (2019): Situation des ressources en eau du bassin versant de la Macta (nord-ouest Algérien), Techniques – Sciences – Méthodes (in french). https://doi.org/10.1051/tsm/201909065

SRTM (Shuttle Radar Topography Mission), https://lpdaac.usgs.gov/products/astgtmv003/

Touaibia, B. (2000): Erosion transport solide -envasement de barrages. Cas du bassin versant del'oued Mina. Thèse de Doctorat d'Etat, INA, El-Harrach, Algérie (in french).

Toubal, A. K., Achite, M., Ouillon, S., Dehni, A. (2018): Soil erodibility mapping using the RUSLE model to prioritize erosion control in the Wadi Sahouat basin, North-West of Algeria. Environ MonitAssess. https://doi.org/10.1007/s10661-018-6580-z

Toumi, S., Meddi, M., Mahé, G., Brou, Y. T. (2013): Cartographie de l'érosion dans le bassin versant de l'Oued Mina en Algérie partélédétection et SIG. Hydrol Sci J 58:1542–1558 (in french). https://doi.org/10.1080/02626667.2013.824088

Wang, G., Wente, S., Gertner, G. Z., Anderson, A. (2002): Improvement in mapping vegetation cover factor for the universal soil loss equation by geostatistical methods with Landsat Thematic Mapper images. Int J Remote Sens 23:3649–3667.

Williams, J. R. (1975): Sediment routing for agricultural watersheds. JAWRA J Am Water Resour Assoc 11: 965–974.

Wischmeier, W. H., Smith, D. D. (1965): Predicting rainfall erosion losses from cropland east of the Rocky Mountains [online]. In: Agricultural Handbook, No. 282. US Department of Agriculture – Agricultural Research Service, Brooksville, 47 p.

Wischmeier, W. H., Smith, D. D. (1978): Predicting rainfall erosion losses- a guide to conservation planning. In: Agriculture Handbook No537. U.S. Department of Agriculture, Washington, DC.

Khadidja Semari, PhD.
Laboratory of Water Sciences and Techniques
University of Mustapha Stambouli Mascara
BP 305 Mamounia Street
Mascara
Algeria

Khaled Korichi, PhD. (*corresponding author, e-mail: kh.korichi@gmail.com)
Laboratory of Civil Engineering and Environment
Djillali Liabes University of Sidi Bel Abbes
BP 89 Sidi Bel Abbes 22000
Algeria